Journal of Electrical and Computer Engineering Innovations
(JECEI)
Journal homepage: http://www.jecei.sru.ac.ir

Research Paper

Cross-correlation based Approach for Counting Nodes of Undersea Communications Network Considering Limited Bandwidth

M. Zillur Rahman [1], ***J. E Giti*** [1,*], ***S. Ariful Hoque Chowdhury*** [2], ***M. Shamim Anower*** [1]

[1]*Department of Electrical & Electronic Engineering, Faculty of Electrical and Computer Engineering, Rajshahi University of Engineering & Technology, Rajshahi, Bangladesh.*

[2]*Department of Electronics & Telecommunication Engineering, Faculty of Electrical and Computer Engineering, Rajshahi University of Engineering & Technology, Rajshahi, Bangladesh.*

Article Info

Article History:
Received 04 September 2024
Reviewed 10 October 2024
Revised 02 November 2024
Accepted 14 November 2024

Keywords:
Bandwidth (BW)
Coefficient of Variation (CV)
Cross-Correlation (CC)
Node counting
Scaling factor (S_F)
Undersea Acoustic Sensor Network (UASN)

*Corresponding Author's Email Address:
jishan.e.giti@gmail.com

Abstract

Background and Objectives: Node counting is undoubtedly an essential task since it is one of the important parameters to maintain proper functionality of any wireless communications network including undersea acoustic sensor networks (UASNs). In undersea communications networks, protocol-based node counting techniques suffer from poor performance due to the unique propagation characteristics of the medium. To solve the issue of counting nodes of an undersea network, an approach based on cross-correlation (CC) of Gaussian signals has been previously introduced. However, the limited bandwidth (BW) of undersea communication presents a significant challenge to the node counting technique based on CC, which traditionally uses Gaussian signals with infinite BW. This article aims to investigate this limitation.

Methods: To tackle the infinite BW issue, a band-limited Gaussian signal is employed for counting nodes, impacting the cross-correlation function (CCF) and the derived estimation parameters. To correlate the estimation parameters for finite and infinite BW scenarios, a scaling factor (S_F) is determined for a specific BW by averaging their ratios across different node counts.

Results: Error-free estimation in a band-limited condition is reported in this work if the S_F for that BW is known. Given the typical undersea BW range of 1–15 kHz, it is also important to establish a relationship between the S_F and BW. This relationship, derived and validated through simulation, allows for determining the S_F and achieving accurate node count under any band-limited condition within the 1–15 kHz range. Furthermore, an evaluation of node counting performance in terms of a statistical parameter called the coefficient of variation (CV) is performed for finite BW scenarios. As a side contribution, the effect of noise on the CC-based undersea node counting approach is also explored.

Conclusion: This research reveals that successful node counting can be achieved using the CC-based technique in the presence of finite undersea BW constraints.

Introduction

In addition to extensive environmental monitoring, undersea acoustic sensor networks (UASNs) are utilized for tasks such as predicting seismic and volcanic activity, offshore exploration, deep-sea archaeology, tactical surveillance, and monitoring oil and gas spills. Ensuring each node in the UASN functions correctly is crucial for these operations. Therefore, counting the operational

nodes in a UASN is required for detecting faulty nodes and maintaining effective network operations, including routing [1] and medium access [2].

The active node number of a UASN can be counted through the cross-correlation (CC) of the Gaussian signals coming from each node. These Gaussian signals are collected by multiple probing nodes called sensors. It is already known that a Gaussian signal has infinite bandwidth (BW). Since no BW constraint is applied to the Gaussian signals coming from each node, the superposition of infinite BW Gaussian signals received at each sensor location is used for node counting. Consequently, this limits the viability of the CC-based scheme in the BW-constrained undersea environment.

The primary objective of this paper is to examine the impact of finite BW on the CC-based technique. This exploration shows error-free node counting through the evaluation of the scaling factor (S_F) for a particular BW. The contributions of this paper are given as follows:

- A band-limited Gaussian signal is employed for counting nodes to investigate the corresponding effect on the cross-correlation function (CCF) and the derived estimation parameters.
- Successful estimation in a BW-constrained condition is demonstrated if the S_F for that BW is known.
- A mathematical expression is derived and validated through simulation for determining the S_F and achieving accurate node count under any finite band condition within the undersea BW range.
- An analysis of node counting error in terms of a statistical parameter called the coefficient of variation (CV) is conducted for varying BW.
- The noise impact on the CC-based undersea node counting method is reported.

A content summary of each subsequent section of the remaining article is given as follows: An in-depth review of existing node counting approaches can be found in the *Related Works* Section. After that, the *Research Gap* Section mentions the limitations of existing works to highlight further research scopes. Then, a brief overview of CC-based node counting methods for background context is provided in the *Background on Estimation Schemes Using CC* Section. The next two consecutive sections titled *BW Impact* and *Relation Between S_F and BW* present explorations of CC-based schemes in finite BW conditions through a mathematical relationship between S_F and BW. The succeeding *Performance Metric* Section discusses the calculation process to determine the counting error parameter and the dependency of that parameter on BW. All mathematical relationships derived throughout the paper are verified in the *Results and Discussion* Section through simulation. Finally, the *Conclusion* Section summarizes the findings of the paper with future directions.

Related Works

To justify the need for a CC based node counting technique, an overview of various estimation procedures for different types of networks is provided in this section. One such early research article by Varagnolo et al. [3] explored distributed anonymous strategies for estimating network cardinality. However, the feasibility of this strategy in wireless networks is yet to be investigated. Later, several algorithms for node estimation in different wireless networks, including wireless sensor and heterogeneous wireless networks, have been developed [4]-[7] without considering the dynamic behavior of the network. In contrast, Cattani et al. [8] introduced Estreme, a neighborhood cardinality estimator designed for dynamic wireless networks.

Apart from the dynamic behavior, network anonymity is another important factor to consider while counting nodes. With this in mind, some researchers work on size estimation methods for anonymous networks based on consensus [9]-[11]. On the other hand, Manaseer et al. [12] conducted a recent study to count the nodes using the mean number of hops required for each exchanged message in mobile ad-hoc networks. Another recent research work by Chatterjee et al. [13] investigated the issue of node number estimation in sparse networks with Byzantine nodes. Nonetheless, the applicability of these terrestrial communication-based node counting methods mentioned so far in undersea communications as well as radio frequency identification (RFID) networks requires further investigation.

RFID technology offers an affordable and flexible solution for object identification. The applications of this technology include the localization and tracking of objects in the supply chain, animal identification, ensuring secure operations in dangerous environments, facilitating electronic payments, and production control. In an RFID system, there are two main parts: a large number of tags for each object and several readers to identify those tags. Tag estimation of an RFID network is equivalent to the node counting in dynamic wireless networks. Since tag counting is a well-studied topic, numerous protocols and schemes for this task can be found in the literature. Recent protocols and schemes for tag counting include the single slot reuse protocol [14], the reliable missing tag estimation protocol [15], the coloring graph-based estimation scheme [16], and the cell averaging constant false alarm rate scheme [17].

RFID is also widely used in the Internet of Things (IoT) where communication overhead is one of the main challenges for active node counting. To address this, an algorithm known as approximate cardinality estimation [18] is utilized for large-scale IoT networks. In

another attempt to boost the node counting scalability for direct-to-satellite IoT networks, Parra et al. [19] proposed an optimistic collision information-based estimator. But, these solutions require significant effort to be developed and further improved. For this reason, machine learning classifiers and artificial neural networks have been introduced recently to tackle the cardinality estimation problem in RFID and IoT networks [19]-[23] which offers competitive performance with reduced design effort. However, all the abovementioned techniques lack the consideration of distinct aspects of undersea acoustic channel (UAC) such as significant capture effect, high path loss, and variable propagation delays, making them unsuitable for undersea environments [24].

A few investigations attempted to overcome the issues of UAC including capture effect. The capture effect refers to the phenomenon where one signal with a received power higher than those of interfering signals by a threshold amount is correctly received by the receiver. Thus, weak signals are not received in the presence of stronger interfering signals. With this in mind, Nemati et al. [25] accounted for the capture effect in tag estimation but did not address other challenges of UAC. A more comprehensive solution considering long propagation delays on top of the capture effect is provided by Howlader et al. [26]-[28] for estimating underwater network size. Blouin [29] also explored a size and structure estimation method based on node-to-node intermissions, enabling distributed computation in underwater networks. The protocol dependency of these methods [26]-[29] adds complexity to undersea network node estimation, making practical implementation difficult. To tackle the problem of protocol complexity in estimating underwater network size, Anower et al. [30]-[33] and Chowdhury et al. [34], [35] propose a new CC-based scheme utilizing two and three probing nodes (sensors), respectively. These schemes employ a straightforward probing protocol and are unaffected by the capture effect. Several assumptions underpin these techniques, including same received power (SRP) from each node, unity signal strength, infinite signal length, and ideal channel conditions (infinite bandwidth, no multipath propagation, and zero Doppler shift). While the SRP can be achieved through the probing technique, practical challenges in UAC such as finite bandwidth, multipath propagation delay, and Doppler shift require further examination. Previous studies have already explored the impacts of signal length [36]-[38], signal strength [39], multipath propagation delay [39]-[42], and dispersion coefficient [43].

Research Gap

Initially, these techniques [30]-[35] use CC of infinite bandwidth Gaussian signals. Later, further research [44], [45] shows the suitability of band-limited (10kHz and 5kHz) Gaussian signals. Scaling factors for 5kHz and 10kHz bandwidths are derived in [44] and [45] for efficient estimation only in these two limited bandwidth scenarios. However, a more general solution is required for any band-limited condition. To achieve this, scaling factors are derived in this paper for the entire underwater bandwidth, considering the finite bandwidth of UAC with two and three sensors to establish a relationship between S_F and bandwidth.

Background on Estimation Schemes Using CC

So far, three estimation schemes have been investigated using CC. They are two-sensor scheme [30]-[33], three-sensor schemes with SL (sensors in line) approach [34] and TS (triangular sensors) approach [35].

System models of these estimation schemes are shown in Fig. 1, where *N* nodes are uniformly distributed across 3D spherical regions underwater but sensor arrangements are different for each case.

In Fig. 1(a), the sensors are located with separation distance, d_{DBS} for two-sensor scheme such that, the distances between the centre of the sphere and the sensors are equal. In SL case, the middle sensor (H_2) is placed at the sphere centre and the other two sensors (H_1 and H_3) are positioned along a line with H_2 such that, $d_{\mathrm{DBS}_{12}}$ (distance between H_1 and H_2) = $d_{\mathrm{DBS}_{23}}$ (distance between H_2 and H_3) = dDBS which is obvious from Fig. 1(b).

In TS scheme, three sensors are positioned such that, $d_{\mathrm{DBS}_{12}} = d_{\mathrm{DBS}_{23}} = d_{\mathrm{DBS}_{31}}$ (distance between *H3* and *H1*) = dDBS to form an equilateral triangle, where the centroid of the triangle lies at the sphere centre which can be visualized in Fig. 1(c). Please note that it is also possible to perform node estimation with random placement of the sensors and different or unequal spacing between the sensors [46]-[48].

The estimation procedure initiates as sensors emit probe requests to *N* nearby nodes. These *N* nodes are treated as acoustic signal emitters capable of transmitting Gaussian signals in reply. When these signals reach the sensors, they arrive in various delayed and attenuated forms and are combined at each sensor location, resulting in mixed Gaussian signals. Through the operation of CC between these signals, CC functions (CCFs) are computed, which manifest as a series of delta functions [30]. For the two-sensor scheme, one CCF is obtained from the CC of the two mixed Gaussian signals received at the two sensor locations. For the SL scheme, two CCFs are derived from the CC of the two signals received by H_1 and H_2 sensors, and, H_2 and H_3 sensors. In the TS scheme, three CCFs are produced from the CC of the two signals received at three pairs of equidistant sensor locations.

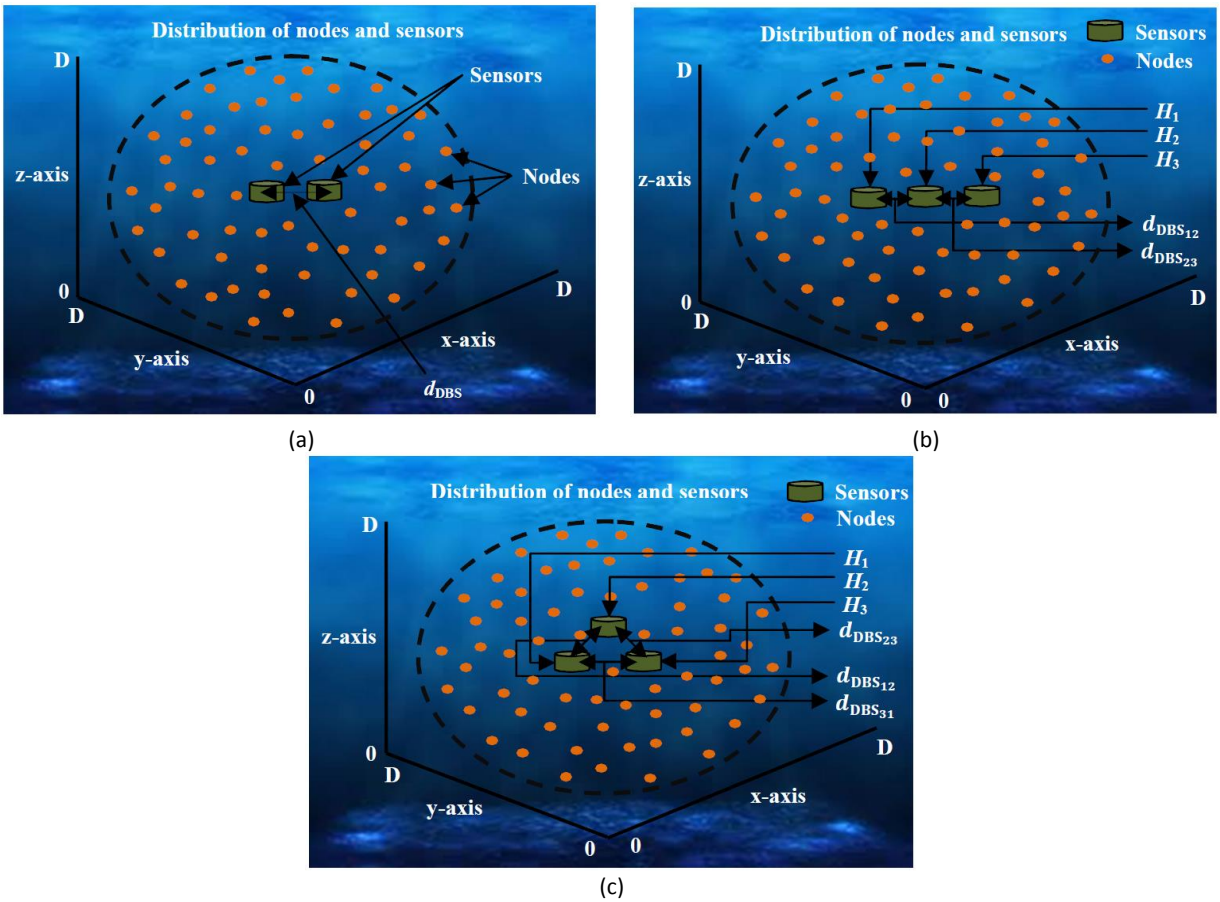

Fig. 1: System models with *N* transmitting nodes for counting the nodes of undersea wireless sensor network: (a) two-sensor method; (b) SL method; and (c) TS method

Fig. 2 illustrates a CCF derived from a network of *N* (=1000) nodes. In this context, bins, denoted as *b*, represent areas where deltas with identical delay variances are situated within a space twice as wide as the sensor spacing. The arrangement of deltas within these bins is dictated by the difference in signal delay experienced by the sensors. Number of bins, *b* is written as follows [49]:

$$b = \frac{2 \times d_{DBS} \times S_R}{S_P} - 1 \tag{1}$$

where, S_P is the speed of acoustic wave propagation and S_R is the sampling rate.

According to [49] and [50], the most preferred parameter for determining the node number using CC based schemes is calculated by taking the ratio between the standard deviation (σ (and the mean (μ (of a CCF. For scenarios with multiple CCFs, such as in the SL and TS cases, several parameters can be acquired, and the ultimate parameter to count the nodes is computed through the averaging of these values. The complex procedure for statistical computation of σ and μ of the CCF can be simplified by treating the CC formulation problem as a probabilistic problem [31].

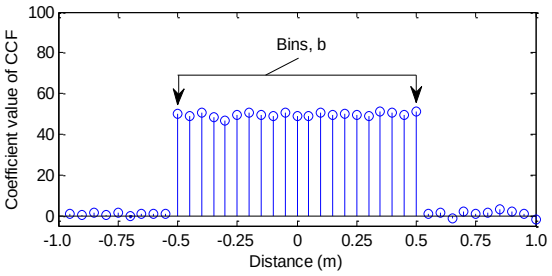

Fig. 2: Bins, *b* of the CCF.

This remodeling is derived from the fact that the bin number of a CCF follows a binomial probability distribution. Now, considering the infinite BW of Gaussian signals, the node counting parameters of two-sensor scheme, SL scheme and TS scheme is written after reformulation from [30], [34] and [35] as:

$$R^{1CCF}_{infiniteBW} = \frac{\sigma}{\mu} = \sqrt{\frac{(b-1)}{N}} \tag{2}$$

$$R^{2CCF}_{infiniteBW} = \frac{R_{12} + R_{23}}{2} = \sqrt{\frac{(b-1)}{N}} \tag{3}$$

and

$$R_{\text{infiniteBW}}^{\text{3CCF}} = \frac{R_{12} + R_{23} + R_{31}}{3} = \sqrt{\frac{(b-1)}{N}} \quad (4)$$

respectively, where R_{12} and R_{23} are the two node counting parameters of SL scheme and R_{12}, R_{23} and $R_{31}$are the three node counting parameters of TS scheme.

Node number, N can be calculated from (2), (3) and (4) for all three methods since estimation parameters are computed using the CCFs and b is determined from S_R, d_{DBS} and S_P using (1).

For 10kHz BW, estimation parameters for two-sensor case and SL case can be expressed from [44] and [45] as:

$$R_{\text{finiteBW}}^{\text{1CCF}} = 0.8093 \times R_{\text{infiniteBW}}^{\text{1CCF}} \quad (5)$$

and

$$R_{\text{finiteBW}}^{\text{2CCF}} = 0.8151 \times R_{\text{infiniteBW}}^{\text{2CCF}} \quad (6)$$

respectively, where 0.8093and 0.8151are the scaling factors. These values are obtained by taking the average of the ratios of R_{finiteBW} for 10kHz to the $R_{\text{infiniteBW}}$ for different N.

From (5) and (6), generalized expressions of estimation parameters for the three estimation schemes in finite BW conditions can be obtained using (2), (3) and (4) as follows:

$$R_{\text{finiteBW}}^{\text{1CCF}} = S_{\text{F}}^{\text{1CCF}} \times \sqrt{\frac{(b-1)}{N}} \quad (7)$$

$$R_{\text{finiteBW}}^{\text{2CCF}} = S_{\text{F}}^{\text{2CCF}} \times \sqrt{\frac{(b-1)}{N}} \quad (8)$$

$$R_{\text{finiteBW}}^{\text{3CCF}} = S_{\text{F}}^{\text{3CCF}} \times \sqrt{\frac{(b-1)}{N}} \quad (9)$$

where, $S_{\text{F}}^{\text{1CCF}}$, $S_{\text{F}}^{\text{2CCF}}$and $S_{\text{F}}^{\text{3CCF}}$ are the scaling factors of two-sensor approach, SL approach and TS approach, respectively.

Relation between S_F and BW

To investigate the dependency of S_F on BW in two-sensor scheme, values of $S_{\text{F}}^{\text{1CCF}}$ for different BW considering the BW range of undersea acoustic communication (15–1kHz) are obtained with b) 19 = S_R = 30kSa/s and d_{DBS}0.5 = m) as shown in Table 1. These values of $S_{\text{F}}^{\text{1CCF}}$ are plotted against BW using linear and log-log scale in Fig. 3(a) and 3(b), respectively.

A straight line equivalence of the $S_{\text{F}}^{\text{1CCF}}$ versus BW curve is presented in Fig. 3(b) where the approximate value of the slant of that straight line is .0.5221Since. Fig. 3(b) is a logarithmic plot, the $S_{\text{F}}^{\text{1CCF}}$ is written as:

$$\log_{10}(S_{\text{F}}^{\text{1CCF}}) = 0.5221 \times \log_{10}(\text{BW}) + k$$

$$\Rightarrow \log_{10}(S_{\text{F}}^{\text{1CCF}}) = \log_{10}(\text{BW})^{0.5221} + \log_{10}(k_3)$$

$$\Rightarrow S_{\text{F}}^{\text{1CCF}} = k_3 \times \text{BW}^{0.5221} \quad (10)$$

Here k and k_3 are constants. Their relationship is given as $k = \log_{10}(k_3)$. The constant k_3 is determined by putting the values of a point from Fig. 3(a) into (10). Thus, the approximate value of k_3 is obtained as 0.0066.

Consequently, the final expression relating S_F and BW for two sensor approach is rewritten using (10) as:

$$S_{\text{F}}^{\text{1CCF}} = 0.0066 \times \text{BW}^{0.5221} \quad (11)$$

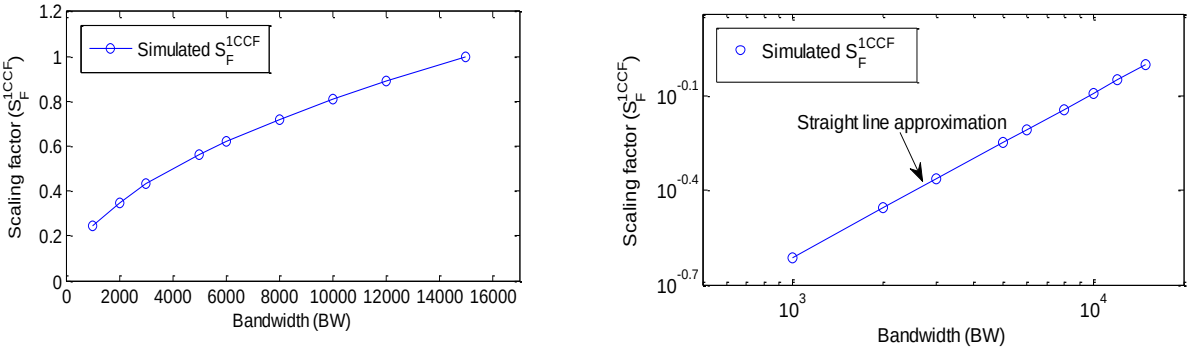

(a) (b)

Fig. 3: Linear (a) and logarithmic (b) plot of $S_{\text{F}}^{\text{1CCF}}$with respect to BW for two-sensor scheme.

Table 1: Scaling factor, $S_{\text{F}}^{\text{1CCF}}$ of two-sensor scheme

BW	1kHz	2kHz	3kHz	5kHz	6kHz	8kHz	10kHz	12kHz	15kHz
$S_{\text{F}}^{\text{1CCF}}$	0.2431	0.3491	0.4315	0.5633	0.6196	0.7200	0.8093	0.8898	1.000

Similarly, Table 2 and 3 contain the values of S_F^{2CCF} and S_F^{3CCF} for SL and TS cases, respectively, with different BW using b .19 = These values are plotted in Fig. 4, where Fig. 4(a) and (b) represent the linear and logarithmic plot of S_F^{2CCF} versus BW, respectively, and Fig. 4(c) and (d)4 represent the linear and logarithmic plot of S_F^{3CCF} versus BW, respectively.

From the straight line approximations as shown in Fig. 4(b) and 4(d), the slopes of the lines are obtained approximately as 0.4956and 0.4608and the values of the intercepts are 0.0085and 0.0119, respectively.

Therefore, S_F^{2CCF} of SL case and S_F^{3CCF} of TS case can be expressed as:

$$S_F^{2CCF} = 0.0085\times BW^{0.4956} \quad (12)$$

and

$$S_F^{3CCF} = 0.0119\times BW^{0.4608} \quad (13)$$

respectively.

Now, putting the expressions of S_F^{1CCF} ,S_F^{2CCF} and S_F^{3CCF} from (11), (12) and (13) into (7), (8) and (9), respectively, the estimation parameters, $R_{\text{finiteBW}}^{1CCF}$ of two sensor

Table 2: Scaling factor, S_F^{2CCF} of SL scheme

BW	1kHz	2kHz	3kHz	5kHz	6kHz	8kHz	10kHz	12kHz	15kHz
S_F^{2CCF}	0.2607	0.3676	0.4494	0.5789	0.6337	0.7308	0.8162	0.8934	1.000

Table 3: Scaling factor, S_F^{3CCF} of TS scheme

BW	1kHz	2kHz	3kHz	5kHz	6kHz	8kHz	10kHz	12kHz	15kHz
S_F^{3CCF}	0.2870	0.3951	0.4762	0.6026	0.6554	0.7483	0.8294	0.9021	1.000

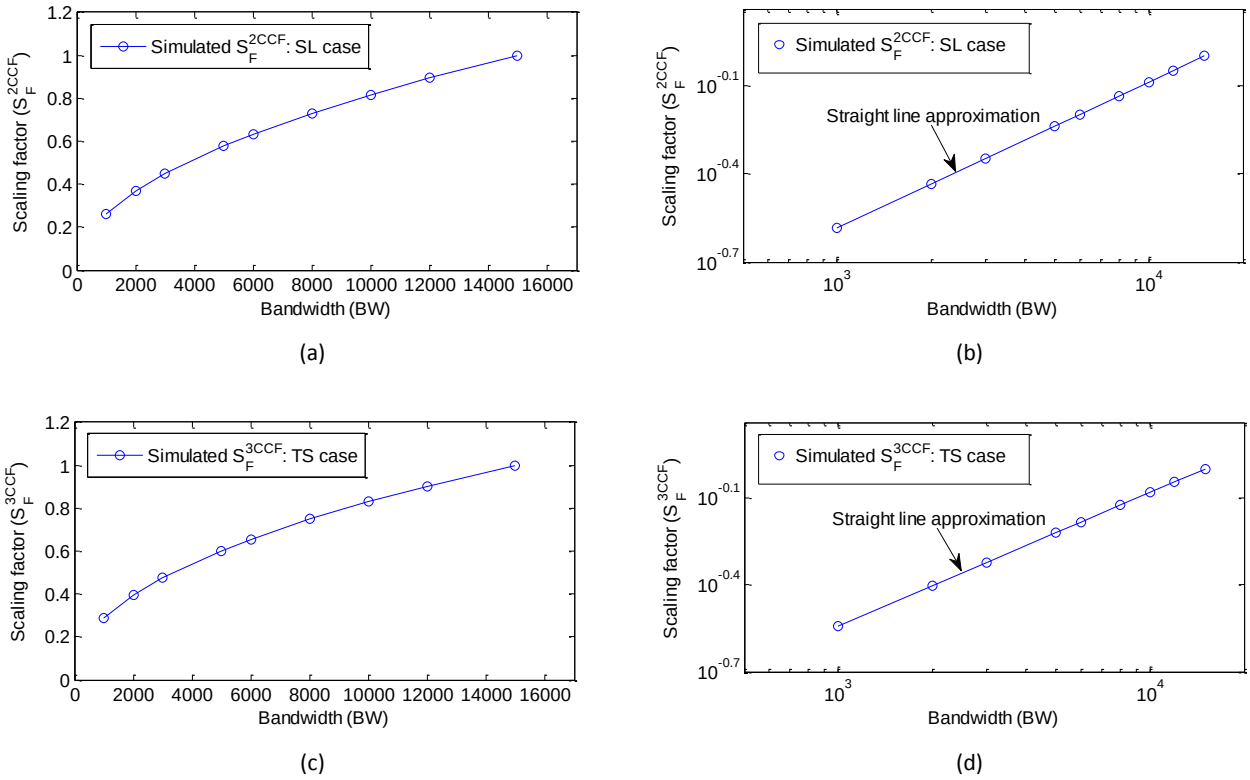

Fig. 4 : S_F^{2CCF} versus BW plot for SL approach in (a) normal; and) b) logarithmic scale and S_F^{3CCF} versus BW plot for TS approach in (c) normal; and (d) logarithmic scale.

scheme, $R_{\text{finiteBW}}^{\text{2CCF}}$ of SL scheme and $R_{\text{finiteBW}}^{\text{3CCF}}$ of TS scheme in finite BW conditions can be expressed as:

$$R_{\text{finiteBW}}^{\text{1CCF}} = 0.0066 \times \text{BW}^{0.5221} \times \sqrt{\frac{(b-1)}{N}} \tag{14}$$

$$R_{\text{finiteBW}}^{\text{2CCF}} = 0.0085 \times \text{BW}^{0.4956} \times \sqrt{\frac{(b-1)}{N}} \tag{15}$$

and

$$R_{\text{finiteBW}}^{\text{3CCF}} = 0.0119 \times \text{BW}^{0.4608} \times \sqrt{\frac{(b-1)}{N}} \tag{16}$$

respectively. Using these relationships, N can be estimated in the three estimation schemes with different BW conditions.

Performance Metric

Due to the statistical nature of the CC-based scheme, a statistical error parameter called coefficient of variation (CV) [51] is used as the performance indicator. CV is calculated by taking the ratio between the standard deviation (σ (and the mean (μ from obtained (several estimated N.

The expression of CV corresponding to the first iteration can be written as follows [52], [53]:

$$\text{CV}_1(N) = \frac{\sigma_1(N)}{\mu_1(N)} \tag{17}$$

Since the standard deviation of a set of estimated N decreases after each iteration of CV calculation, the $\text{CV}_\text{u}(N)$ corresponding to uth iteration is $1/\sqrt{u}$ times smaller than that of the first iteration [54], [55]. Now, we can rearrange (7), (8) and (9) as:

$$N = (b-1) \times \left(\frac{S_\text{F}^{\text{1CCF}}}{R_{\text{finiteBW}}^{\text{1CCF}}}\right)^2 \tag{18}$$

$$N = (b-1) \times \left(\frac{S_\text{F}^{\text{2CCF}}}{R_{\text{finiteBW}}^{\text{2CCF}}}\right)^2 \tag{19}$$

$$N = (b-1) \times \left(\frac{S_\text{F}^{\text{3CCF}}}{R_{\text{finiteBW}}^{\text{3CCF}}}\right)^2 \tag{20}$$

to obtain the expressions to determine N for two-sensor approach, SL approach and TS approach, respectively. By putting these expressions of N into (17), the CVs (after u iterations) for the three estimation schemes can be written as:

$$\text{CV}_{\text{finiteBW}}^{\text{1CCF}}(N) = \frac{1}{\sqrt{u}} \frac{\sigma_\text{u}\left((b-1)\left(\frac{S_\text{F}^{\text{1CCF}}}{R_{\text{finiteBW}}^{\text{1CCF}}}\right)^2\right)}{\mu_\text{u}\left((b-1)\left(\frac{S_\text{F}^{\text{1CCF}}}{R_{\text{finiteBW}}^{\text{1CCF}}}\right)^2\right)} \tag{21}$$

$$\text{CV}_{\text{finiteBW}}^{\text{2CCF}}(N) = \frac{1}{\sqrt{u}} \frac{\sigma_\text{u}\left((b-1)\left(\frac{S_\text{F}^{\text{2CCF}}}{R_{\text{finiteBW}}^{\text{2CCF}}}\right)^2\right)}{\mu_\text{u}\left((b-1)\left(\frac{S_\text{F}^{\text{2CCF}}}{R_{\text{finiteBW}}^{\text{2CCF}}}\right)^2\right)} \tag{22}$$

$$\text{CV}_{\text{finiteBW}}^{\text{3CCF}}(N) = \frac{1}{\sqrt{u}} \frac{\sigma_\text{u}\left((b-1)\left(\frac{S_\text{F}^{\text{3CCF}}}{R_{\text{finiteBW}}^{\text{3CCF}}}\right)^2\right)}{\mu_\text{u}\left((b-1)\left(\frac{S_\text{F}^{\text{3CCF}}}{R_{\text{finiteBW}}^{\text{3CCF}}}\right)^2\right)} \tag{23}$$

where, the CVs corresponding to two-sensor scheme, SL scheme and TS scheme are represented by $\text{CV}_{\text{finiteBW}}^{\text{1CCF}}(N)$, $\text{CV}_{\text{finiteBW}}^{\text{2CCF}}(N)$ and $\text{CV}_{\text{finiteBW}}^{\text{3CCF}}(N)$, respectively. It is obvious from (21), (22) and (23) that the CVs vary with b and scaling factors as well as BW.

Results and Discussion

This section contains all results related to node counting and performance comparison in three subsections. The results of the first two subsections correspond to node counting in the presence of noise and limited BW conditions. The third subsection reports counting errors in terms of CV.

Node counting in the presence of noise: To show the effect of noise, the internal noise of the receivers (sensors) is added to the node counting process. At first, the effect of noise on the two-sensor scheme is shown considering additive white Gaussian noise (AWGN) as the internal noise of a receiver. Simulations are conducted using the MATLAB programming tool, with varying signal ,lengthN_S (varies from 10^3 to 10^6samples) and signal-to-noise ratio, SNR, (varies from 10^{-5} to 10^5) of the receivers for a certain number (32 in this case) of nodes.

Other parameters used in the simulations (throughout the work unless otherwise mentioned) are: sphere dimension, 200D = 0m; sampling rate, S_R = 60kSa/s (because underwater acoustic bandwidth is around 15 kHz, this sampling rate is considered without violating the sampling theorem); speed of propagation, S_P = 1500m/s (typical underwater sound velocity); distance between sensors, d_{DBS} = 0.5m (so that the estimation sensors remain at the one node); absorption coefficient, a = 1 and dispersion factor, k = 1.5 (these are typical values for underwater acoustic communication). Results are plotted in Fig. 5, which presents the surface plots of N, SNR and N_S.

It can be seen in the results that, for a particular signal length (for example 100,000 samples) up to a certain SNR (<=0.05), the estimation is constant at the worst possible value but then improves with increases in SNR (up to SNR = 1).

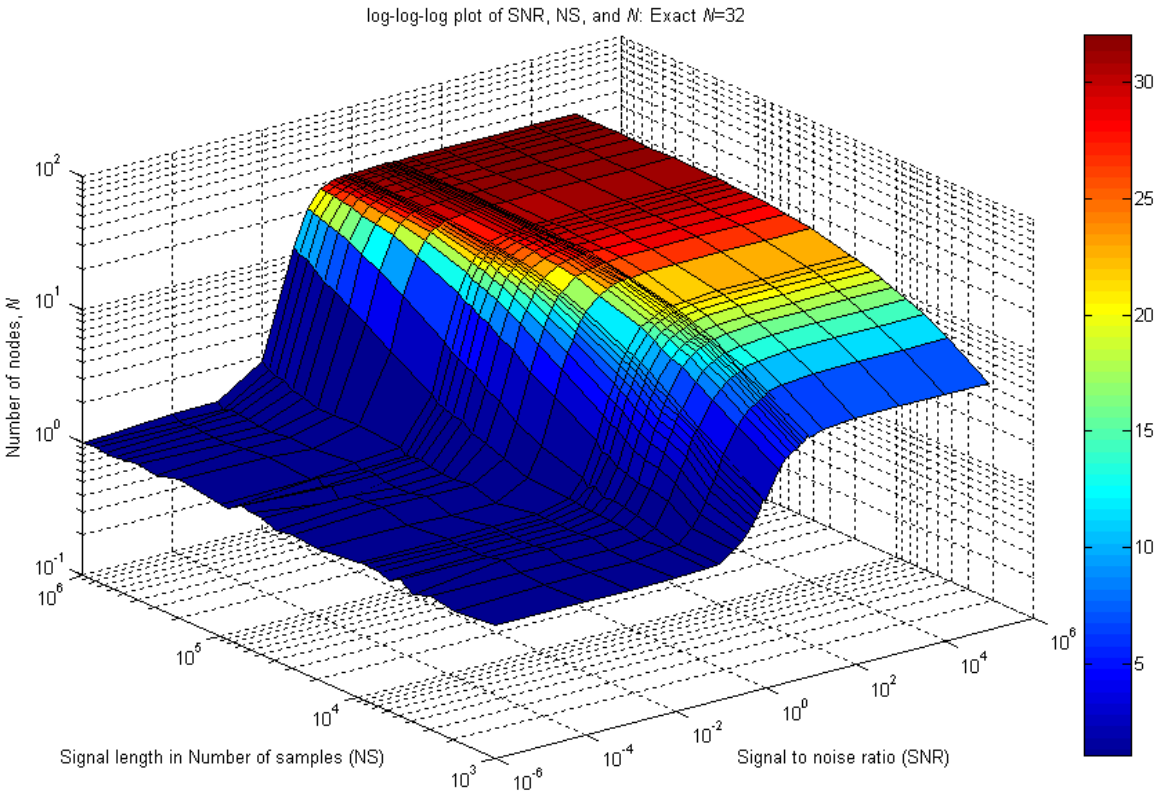

Fig. 5: Surface plot of SNR (10^{-5} to 10^{5}), N_S (10^3 to 10^6samples) and N (ideally 32) in logarithmic scale for two-sensor scheme.

Finally, the estimation becomes constant again at the maximum value, which corresponds to the case without noise. That is: when the SNR is less than 1, although the noise dominates over the signal, there are some signals that are strong enough to count; and, although we cannot estimate the appropriate number, we receive a reduced number of the signal sources, i.e., nodes. It can also be seen from Fig. 5 that, there is a transition zone between the worst and best possible values in which the estimation is varied with the SNR whose start and end points are varied with the signal length, i.e., it will start earlier with a greater signal length and later with a shorter signal length.

In a noisy environment, the transmitted signal must have sufficient power such that a suitable SNR is achieved. The effect of noise also varies with signal length (which determines the integration time of the cross-correlation process), the greater the length, the less is the effect of noise. This investigation shows that, if the signal strength and length are chosen properly, the estimation performance is similar to that of the ideal (without noise) case. It also shows that a SNR of 20 dB is sufficient to receive the signal with no errors as well as to neglect the noise effect in the estimation process.

Similar conclusions can be drawn for SL and TS schemes TS schemes and as the effect of noise will be similar for all three schemes.

Node counting with finite BW: The theoretical relationship between SF and BW, developed in one of the previous sections, is verified here through simulation work. Simulation results of $R^{1CCF}_{\text{finiteBW}}$,$R^{2CCF}_{\text{finiteBW}}$ and $R^{3CCF}_{\text{finiteBW}}$ for two-sensor, SL and TS approaches with corresponding theoretical results using (14), (15) and (16) are shown in Fig. 6(a), 6(b) and 6(c), respectively, using b = 39; and in Fig. 7(a), 7(b) and 7(c), respectively, using b = 89 with 12kHz and 3kHz BW.

In Fig. 6 and 7, the matching results from simulation and theory prove the usefulness of the expressions formulated in the *Relation between* S_F and *BW* Section. The additional simulation parameters are: signal length, Ns = 10^6 samples; signal to-noise ratio, SNR = 20 dB.

To demonstrate the significance of the S_F, Figs. 8, 9 and 10 show plots of the estimated (from simulation by averaging over 500 iterations) versus the exact node number for the two-sensor, SL, and TS approaches, respectively.

The plots include simulations both with and without S_F, along with the theoretically estimated node count using different BW and b values. The values of BW and b are: BW = 12kHz and b = 39 (S_R = 60kSa/s and d_{DBS}= 0.5m) in Fig. 8(a), 9(a), and 10(a); BW = 12kHz and b =89 (S_R = 45kSa/s and d_{DBS} = 1.5m) in Fig. 8(b), 9(b), and 10(b); BW = 3kHz and b = 39 in Fig. 8(c), 9(c), and 10(c) and BW = 3kHz and b = 89 in Fig. 8(d), 9(d) and 10(d).

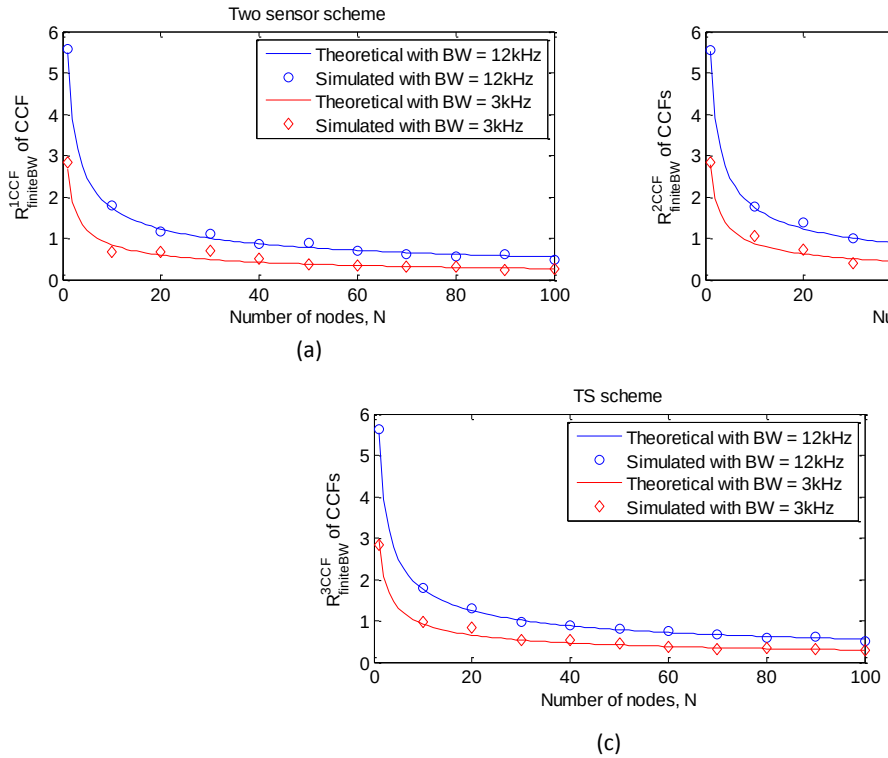

Fig. 6: Estimation parameter: (a) $R^{1CCF}_{finiteBW}$ of two-sensor scheme; (b) $R^{2CCF}_{finiteBW}$ of SL scheme; and (c) $R^{3CCF}_{finiteBW}$ of TS scheme versus *N* plot with BW = 12kHz and BW = 3kHz for b = 39 (d_{DBS} = 0.5m and S_R = 60kSa/s).

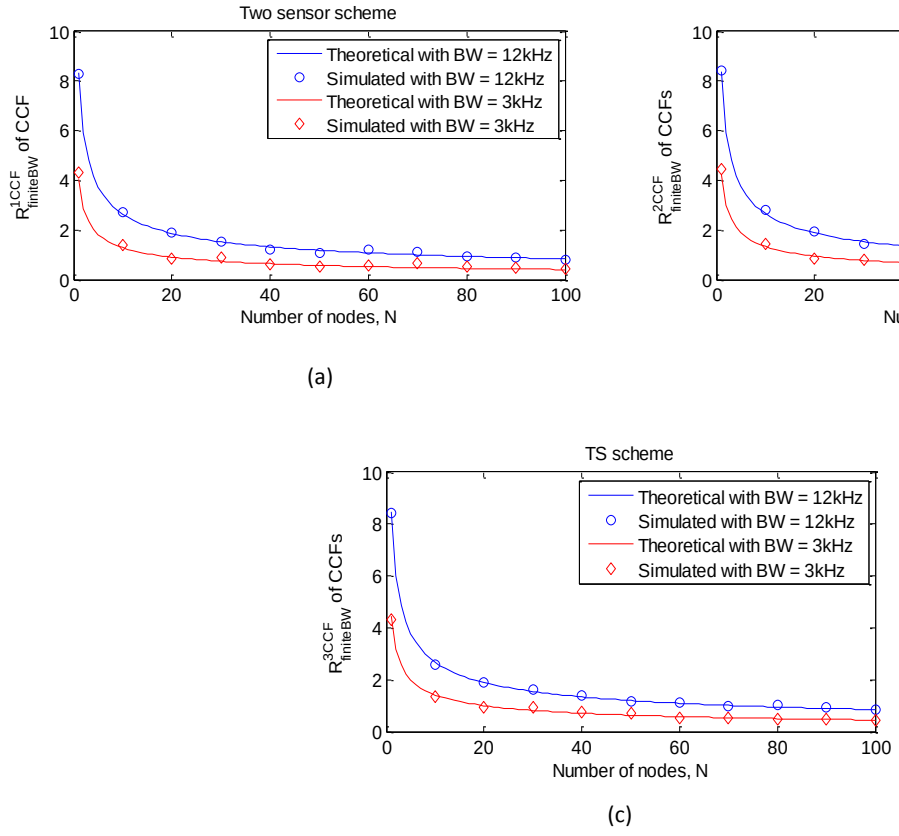

Fig. 7: Estimation parameter: (a) $R^{1CCF}_{finiteBW}$ of two-sensor scheme; (b) $R^{2CCF}_{finiteBW}$ of SL scheme; and (c) $R^{3CCF}_{finiteBW}$ of TS scheme versus *N* plot with BW = 12kHz and BW = 3kHz for b = 89 (d_{DBS} = 1.5m and S_R = 45kSa/s).

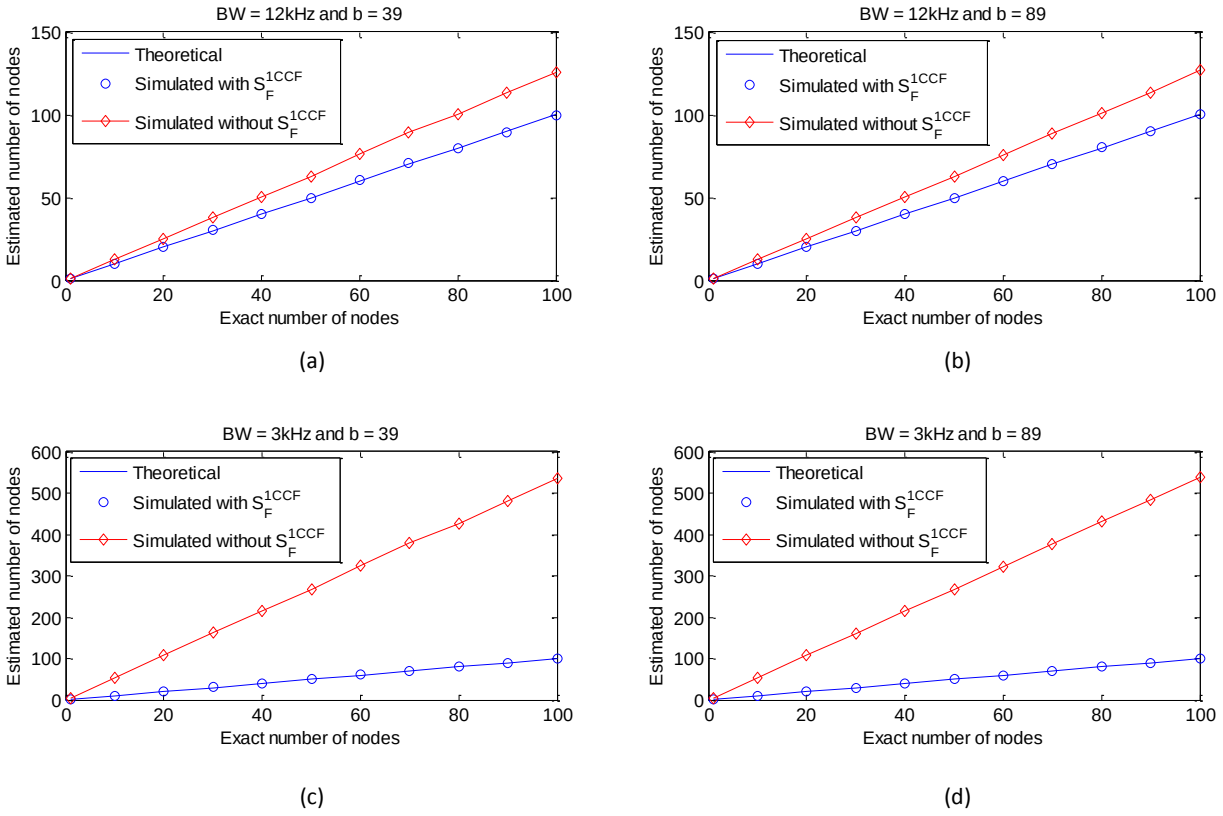

Fig. 8: Comparative analysis of estimated node number obtained from simulation for two-sensor scheme with and without S_F using different bandwidth (BW) and number of bins (b).

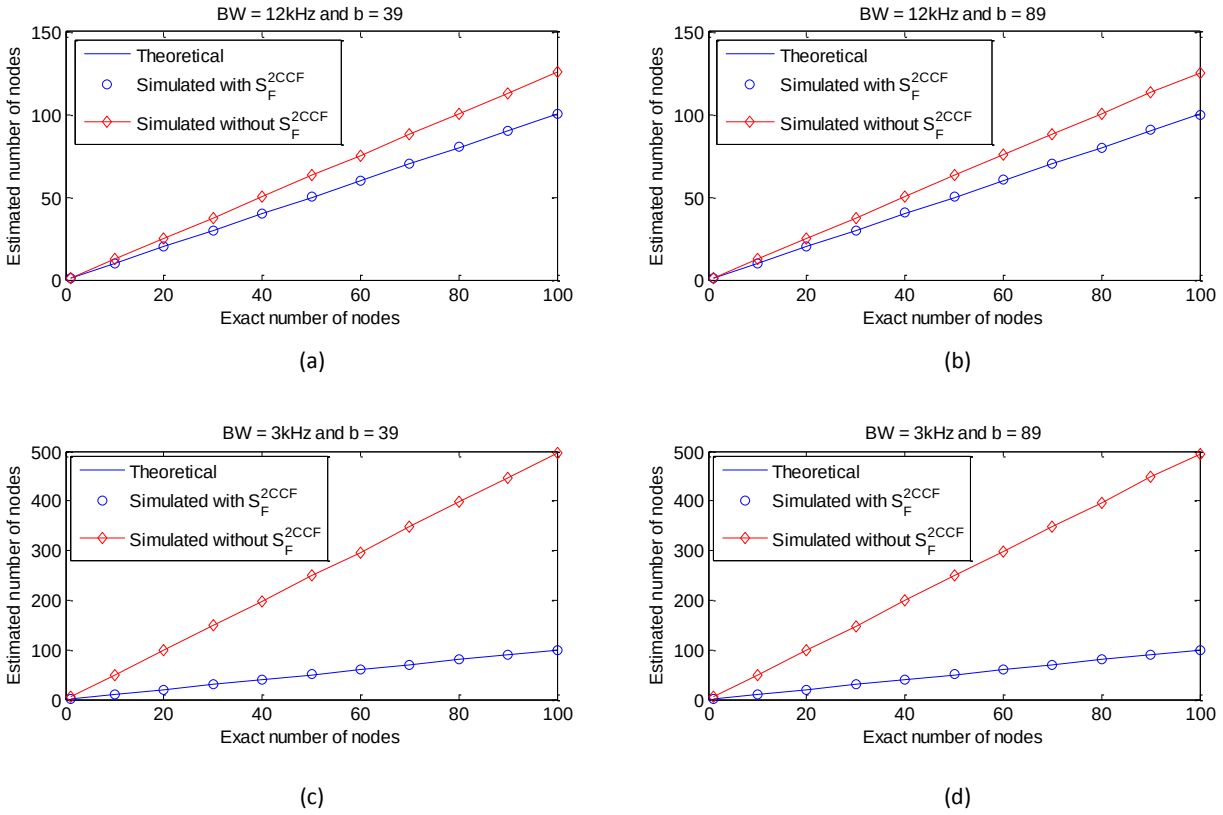

Fig. 9: Comparative analysis of estimated node number obtained from simulation for SL scheme with and without S_F using different bandwidth (BW) and number of bins (b).

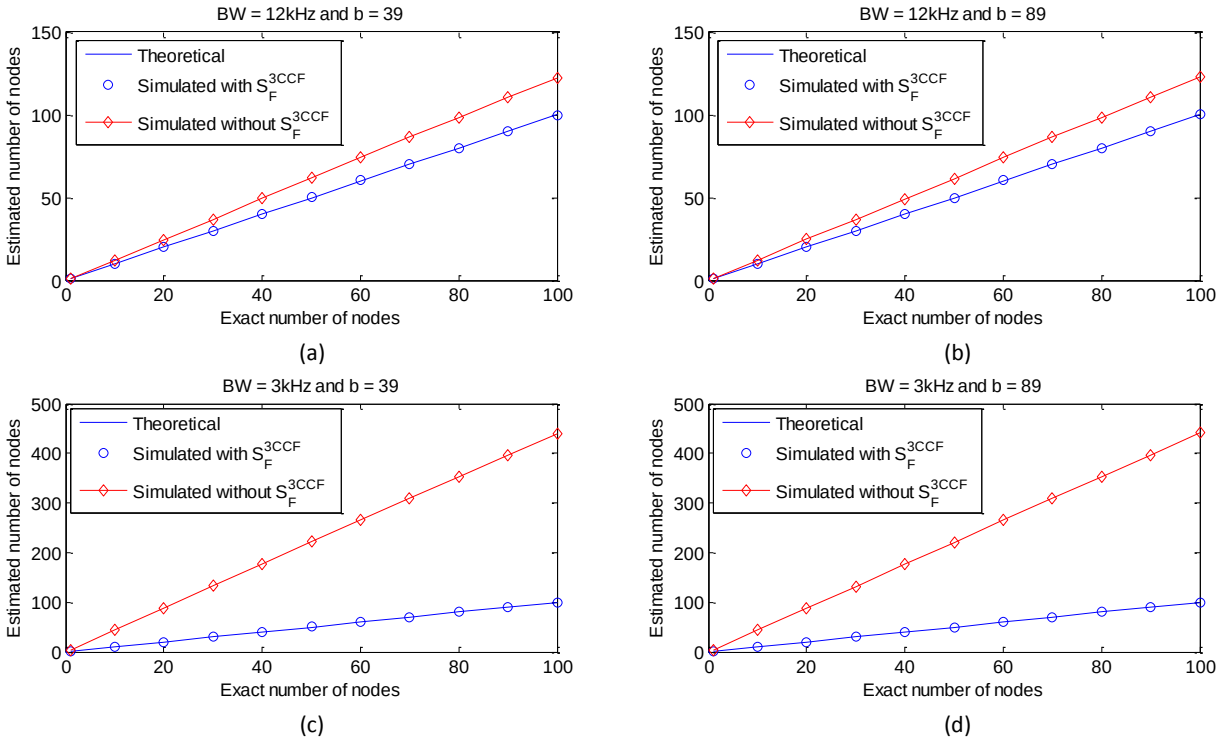

Fig. 10: Comparative analysis of estimated node number obtained from simulation for TS scheme with and without S_F using different bandwidth (BW) and number of bins (b).

It is obvious from all the results presented by Fig. 8, 9 and 10 that, satisfactory estimation can be achieved with S_F in different band-limited conditions using various b. In these plots, simulated node counting results (as shown by blue markers) match the corresponding theoretical results (as shown by blue lines), displaying the adequacy of S_F. It is also clear from these figures that, erroneous estimation (as shown by overlapping red markers and lines) is obtained without S_F in the same band-limited conditions using the same values of b, which indicates the importance of S_F.

Nonetheless, the difference between blue and red lines (as well as markers) in each plot of Fig. 8, 9 and 10 indicates the node counting error caused by limited BW. For without S_F case, this difference and consequently, the estimation error is smaller in the top two plots of each of these figures compared to those of the bottom two plots. Moreover, the top row plots (Fig. 8(a), 8(b), 9(a), 9(b), 10(a) and 10(b)) correspond to a higher BW than that of the bottom row plots (Fig. 8(c), 8(d), 9(c), 9(d), 10(c) and 10(d)). According to these findings, we can say that narrower BW conditions affect the CCFs as well as the estimation parameters derived from those CCFs more significantly than the wider BW cases leading to higher node counting errors. Therefore, the higher the BW, the lower the estimation error, and vice versa.

For further investigation, percentage relative estimation errors (e_r) without using S_F for two-sensor method, SL method and TS method are shown in Fig. 11 using different BW and b to compare the effect of BW on estimation accuracy of these three estimation methods. In Fig. 11, the values of BW and b corresponding to each plot are the same as those of the previous three figures (Fig. 8, 9 and 10). It can be seen from Fig. 11 that, the two-sensor approach shows the maximum e_r and TS approach shows the minimum e_r among the three schemes. Therefore, the SL and TS approaches are less impacted by finite BW than the two-sensor approach. However, the effect of BW is more pronounced in the SL approach compared to the TS approach. Fig. 11 also shows that, e_r increases with the decrease of BW for all three methods. In Fig. 11, fluctuating values of e_r indicate that, it is preferable to calculate statistical error for these schemes in terms of CV.

Node counting error: The performance of CC-based schemes is measured using the CV which provides a statistical node counting error. Due to the inverse relationship between CV and node counting accuracy, higher CV indicates lower accuracy and vice versa. To demonstrate the impact of finite BW on CV, simulation results of $\mathrm{CV}_{\mathrm{finiteBW}}^{1\mathrm{CCF}}(N)$, $\mathrm{CV}_{\mathrm{finiteBW}}^{2\mathrm{CCF}}(N)$ and $\mathrm{CV}_{\mathrm{finiteBW}}^{3\mathrm{CCF}}(N)$ corresponding to 100th iteration for two-sensor, SL and TS approaches are shown in Fig. 12. The plots include simulation results both with and without S_F, using different BW and b values to emphasize the further importance of scaling factors. The chosen values of BW and b of Fig. 12(a), 12(b), 12(c) and 12(d) are the same as those of Fig. 11(a), 11(b), 11(c) and 11(d), respectively, so that a more comprehensive and conclusive analysis of BW impact can be conducted.

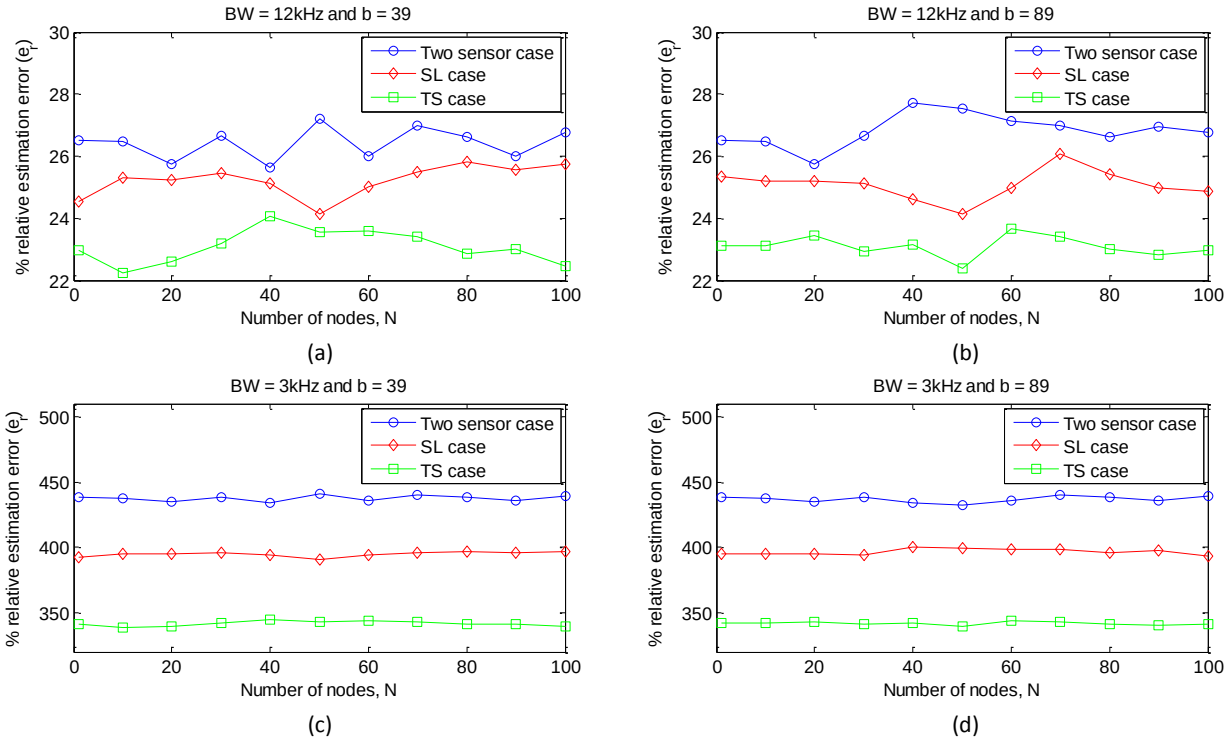

Fig. 11: Comparisons of er in two-sensor, SL and TS methods without using S_F for: (a) BW = 12kHz and b = 39 (dDBS = 0.5m and S_R = 60kSa/s); (b) BW = 12kHz and b = 89 (d_{DBS} = 1.5m and S_R = 45kSa/s); (c) BW = 3kHz and b = 39; and (d) BW = 3kHz and b = 89.

The CVs of Fig. 12 for different schemes and BW scenarios show similar traits as those of the percentage relative estimation errors, e_r of Fig. 11. Similar to e_r, CV also decreases with the increase of BW for all three schemes, and vice versa according to Fig. 12. This similar characteristics of CV and e_r with respect to BW is expected since both of these metrics have a similar dependency on the node counting parameters derived from the inaccurately formed CCFs due to the impact of finite BW condition.

It can be seen from Fig. 12 that, the TS approach shows the minimum CV whereas the two-sensor approach shows the maximum CV among the three methods. The underlying reason for the best node counting performance (corresponding to the lowest CV) achieved by the TS scheme is the use of more (in this case three) estimation parameters. This is because node counting using three (or u number of) parameters is equivalent to counting the nodes three (or u number of) times (or iterations) using a single parameter and since the accuracy of CC-based methods increases with the number of iterations used in the estimation process. Therefore, the performance of two-sensor and SL approaches in terms of CV is more impacted by limited BW conditions than the TS approach. Similarly, the SL approach is more robust compared to the two-sensor approach since two parameters are averaged by the SL scheme while a single node counting parameter is used by the two-sensor scheme. Fig. 12 also shows that the CVs obtained with S_F are lower than those of the corresponding scenarios without S_F. This is quite similar to Fig. 8, 9, and 10 where the lack of using S_F in finite BW conditions leads to inaccurate node counting results. These erroneous results are expected to have higher values of CV compared to those of the corresponding results obtained with S_F. Moreover, higher CVs as a consequence of not using S_F are more noticeable in smaller BW scenarios than in broader BW conditions. Hence, the use of S_F is more critical in lower BW cases.

Conclusion

This work addresses the issue of undersea bandwidth constraints on CC-based node counting schemes. It derives the relationship between scaling factors (S_F) and BW to provide generalized expressions for estimation parameters across three CC-based schemes in finite BW conditions, supported by simulations using various BW and b values. The study demonstrates that efficient estimation is achievable using S_F in limited BW conditions. However, without S_F, significant estimation errors occur which has been evaluated in terms of a statistical parameter called the coefficient of variation. Additionally, it shows that the estimation results of the TS approach are less affected by limited BW compared to the SL and two-sensor approaches. Future goals include analyzing the consequence of various environmental factors such as temperature, salinity, and underwater currents on the estimation performance of these three methods and eliminating other assumptions of CC-based schemes, such as the network's spherical shape and uniform node distribution.

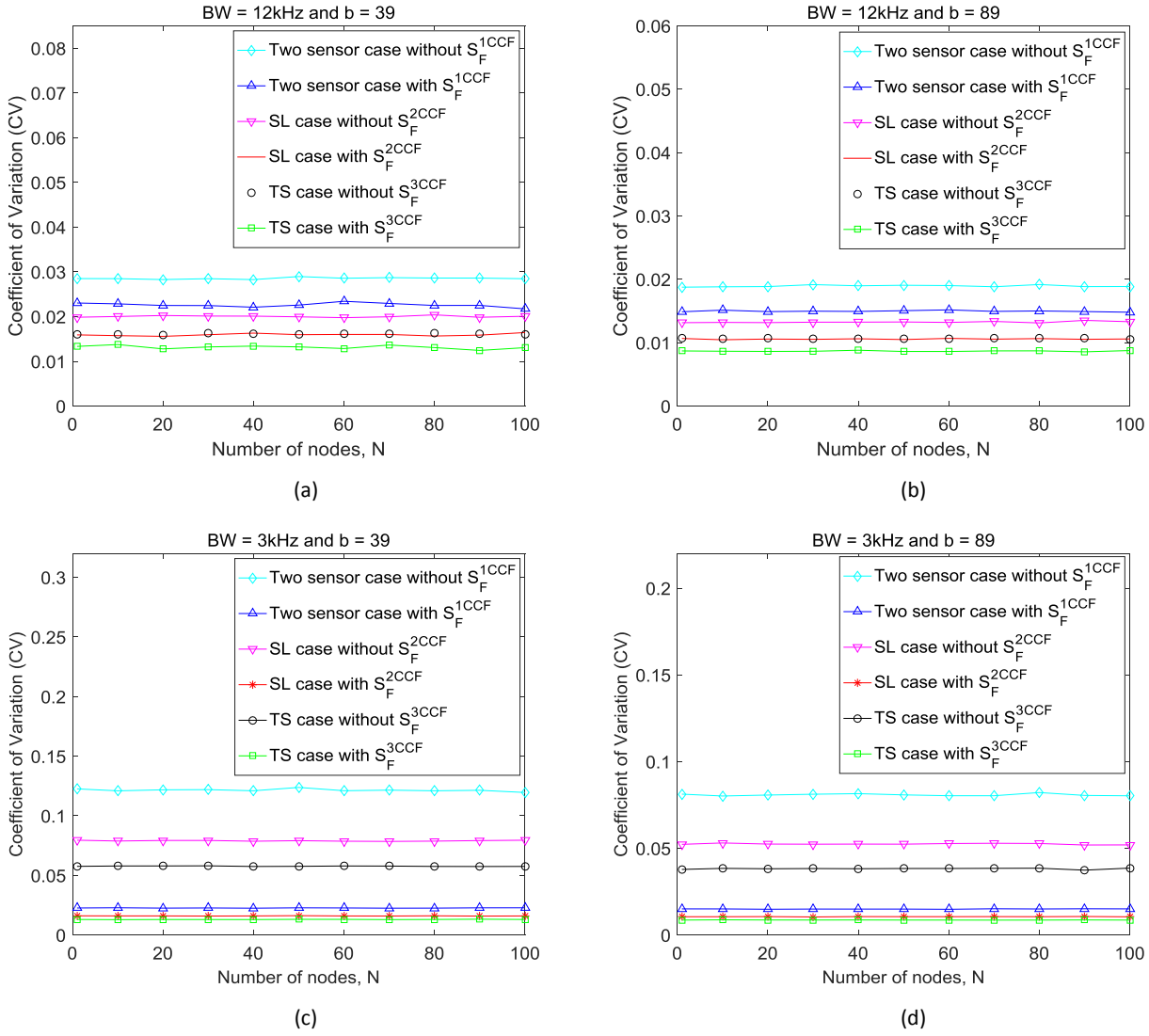

Fig. 12: Node counting performance evaluation in terms of CV of two-sensor, SL and TS methods with and without using S_F for: (a) BW = 12kHz and b = 39 (d_{DBS} = 0.5m and S_R = 60kSa/s); (b) BW = 12kHz and b = 89 (d_{DBS} = 1.5m and S_R = 45kSa/s); (c) BW = 3kHz and b = 39 (d_{DBS} = 0.5m and S_R = 60kSa/s); and (d) BW = 3kHz and b = 89 (d_{DBS} = 1.5m and S_R = 45kSa/s).

Author Contributions

Conceptualization: Shah Ariful Hoque Chowdhury, Md. Shamim Anower; Methodology: Md. Zillur Rahman; Formal analysis and investigation: Md. Zillur Rahman, Jishan E Giti; Writing - original draft preparation: Md. Zillur Rahman, Jishan E Giti; Writing - review and editing: Md. Zillur Rahman, Jishan E Giti; Supervision: Shah Ariful Hoque Chowdhury, Md. Shamim Anower.

Conflict of Interest

The authors declare no potential conflict of interest regarding the publication of this work. In addition, the ethical issues including plagiarism, informed consent, misconduct, data fabrication and, or falsification, double publication and, or submission, and redundancy have been completely witnessed by the authors.

Abbreviations

BW	*Bandwidth*
CV	*Coefficient of Variation*
CC	*Cross-correlation*
CCF	*Cross-correlation Function*
SL	*Sensors in Line*
TS	*Triangular Sensors*
UAC	*Undersea Acoustic Channel*
UASN	*Undersea Acoustic Sensor Network*

References

[1] S. Ashraf, M. Gao, Z. Chen, H. Naeem, T. Ahmed," CED-OR based opportunistic routing mechanism for underwater wireless sensor networks," Wireless Pers. Commun., 125: 487-511, 2022.

[2] G. Cario, A. Casavola, F. Torchiaro, "Medium access control in underwater sensor networks: a comparison between the standard JANUS and Ad-Hoc energy-efficient MAC protocols," in Proc. of the

10th Convention of the European Acoustics Association Forum (Acusticum): 5071-5078, 2023.

[3] D. Varagnolo, G. Pillonetto, L. Schenato, "Distributed Cardinality Estimation in Anonymous Networks," IEEE Trans. Autom. Control, 59(3): 645-659, 2014 .

[4] S. Chen, Y. Qiao, S. Chen, J. Li, "Estimating the cardinlaity of a mobile peer-to-peer network," IEEE J. Sel. Areas Commun., 31(9): 359-368, 2013.

[5] O. Sluciak, M. Rupp, "Network size estimation using distributed orthogonalization," IEEE Signal Processing Lett., 20(4): 347-350, 2013.

[6] A. Douik, S. A. Aly, T. Y. Al-Naffouri, M. S. Alouini, "Cardinality estimation algorithm in large-scale anonymous wireless sensor networks," in Proc. International Conference on Advanced Intelligent System and Informatics: 569-578, 2018.

[7] S. Kadam, K. S. Bhargao, G. S. Kasbekar, "Node cardinality estimation in a heterogeneous wireless network deployed over a large region using a mobile base station," J. Network Comput. Appl., 221: 103779, 2024.

[8] M. Cattani, M. Zuniga, A. Loukas, K. Langendoen, "Lightweight neighborhood cardinality estimation in dynamic wireless networks," in Proc. 13th Int. Symposium Information Processing in Sensor Networks: 179-189 , 2014.

[9] D. Varagnolo, G. Pillonetto, L. Schenato, "Consensus based estimation of anonymous networks size using Bernoulli trials," in Proc. American Control Conf.: 2196-2201, 2012.

[10] G. Luna, R. Baldoni, S. Bonomi, I. Chatzigiannakis, "Conscious and unconscious counting on anonymous dynamic networks," in Proc. International Conference on Distributed Computing and Networking: 257-271, 2014.

[11] R. Lucchese, D. Varagnolo, J. C. Delvenne, J. Hendrickx, "Network cardinality estimation using max consensus: The case of Bernoulli trials," in Proc. 54th IEEE Conference on Decision and Control (CDC): 895-901, 2015.

[12] S. Manaseer, I. Alhabash, "Number of node estimation in mobile Ad Hoc networks," Int. J. Interac. Mob. Technol. (iJIM), 11(6): 65-72, 2017.

[13] S. Chatterjee, G. Pandurangan, P. Robinson, "Network size estimation in small-world networks under byzantine faults," in Proc .IEEE International Parallel and Distributed Processing Symposium (IPDPS): 855-865, 2019.

[14] Z. Xi, X. Liu, J. Luo, S. Zhang, S. Guo, "Fast and reliable dynamic tag estimation in large-scale RFID systems," IEEE Internet Things J., 8(3): 1651-1661, 2021.

[15] B. Wang, G. Duan, "A reliable cardinality estimation for missing tags over a noisy channel," Comput. Commun., 188: 125-132, 2022.

[16] Z. He, "Reader scheduling for tag population estimation in multicategory and multireader RFID systems," Wireless Commun. Mob. Comput., 2021.

[17] A. Frahtia, M. Benssalah, A. Kifouche, K. Drouiche, "Improved tag estimation method for TDMA anticollision protocols using CA-CFAR technique," Frequenz, 78(11-12): 697-708, 2024.

[18] Q. Cao, Y. Feng, Z. Lu, H. Qi, L. M. Tolbert, L. Wan, Z. Wang, W. Zhou, "Approximate Cardinality Estimation (ACE) in large-scale Internet of Things deployments," Ad Hoc Networks, 66: 52-63, 2017.

[19] P. I. Parra, S. M. Sánchez, J. A. Fraire, R. D. Souza, S. Céspedes, "Network size estimation for direct-to-satellite IoT," IEEE Internet Things J., 10(7): 6111-6125, 2023.

[20] X. Jie, L. Haoliang, D. Wei, J. Ao, "Network host cardinality estimation based on artificial neural network," Secur. Commun. Netw., 2022.

[21] L. D. Rodić, I. Stančić, K. Zovko, T. Perković, P. Šolić, "Tag estimation method for ALOHA RFID system based on machine learning classifiers," Electronics, 11(16): 2605, 2022.

[22] P. S. Page, A. S. Siyote, V. S. Borkar, G. S. Kasbekar, "Node cardinality estimation in the internet of things using privileged feature distillation," IEEE Trans. Mach. Learn. Commun. Netw., 2: 1229-1247, 2024.

[23] S. A. Alhuthali, M. Murad, I. A. Tasadduq, M. H. Awedh, A. M. Rushdi, S. Alotaibi, "An effective tag estimation method based upon artificial neural networks and signal strength for anticollision in radio frequency identification systems," Int. J. Comput. Intell. Syst., 17(200), 2024.

[24] S. Climent, A. Sanchez, J. V. Capella, N. Meratnia, J. J. Serrano , "Underwater acoustic wireless sensor networks: Advances and future trends in physical, MAC and routing layers," Sensors (Basel Switzerland), 14(1): 795-833, 2014.

[25] M. Nemati, H. Takshi, V. Shah-Mansouri, "Tag estimation in RFID systems with capture effect," in Proc. 23rd Iranian Conference on Electrical Engineering: 368-373, 2015.

[26] M. S. A. Howlader, M. R. Frater, M. J. Ryan, "Estimation in underwater sensor networks taking into account capture," in Proc. IEEE Oceans'07, Aberdeen, Scotland: 1-6, 2007.

[27] M. S. A. Howlader, M. R. Frater, M. J. Ryan, "Estimating the number of neighbours and their distribution in an underwater communication network," in Proc. Second Int. Conf. Sensor Technologies and Applications, 2007.

[28] M. S. A. Howlader, M. R. Frater, M. J. Ryan, "Delay-insensitive identification of neighbors using unslotted and slotted protocols," Wirel. Commun. Mob. Comput., 2012.

[29] S. Blouin, "Intermission-based adaptive structure estimation of wireless underwater networks," in Proc. 10th IEEE Int. Conf. Networking, Sensing and Control: 146-151, 2013.

[30] S. Anower, M. R. Frater, M. J. Ryan, "Estimation by cross-correlation of the number of nodes in underwater networks," in Proc. Australasian Telecommunication Networks and Applications Conf.: 1-6, 2009.

[31] M. S. Anower, M. A. Motin, A. S. M. Sayem, S. A. H. Chowdhury, "A node estimation technique in underwater wireless sensor network," in Proc. Int .Conf. Informatics, Electronics & Vision: 1–6, 2013.

[32] S. Hossain, A. Mallik, M. A. Arefin, "A signal processing approach to estimate underwater network cardinalities with lower complexity," J. Electr. Comput. Eng. Innovations (JECEI), 5(2): 131-138, 2017.

[33] N. Afrin, S. Anower, M. Islam, "Dimensionality determination of unknown deployed underwater sensor network (UWSN) using cost function," Int. J. Commun. Syst., 33 (15): e4537, 2020.

[34] S. A. H. Chowdhury, M. S. Anower, J. E. Giti, "A signal processing approach of underwater network node estimation with three sensors," in Proc. 1st Int. Conf. Electrical Engineering and Information & Commun. Technology: 1-6, 2014.

[35] S. A. H. Chowdhury, M. S. Anower, J. E. Giti, "Effect of sensor number and location in cross-correlation based node estimation technique for underwater communications network," in Proc. 3rd Int. Conf .Informatics, Electronics & Vision: 1-6, 2014.

[36] M. A. Hossen, S. A. H. Chowdhury, M. S. Anower, S. Hossen, M. F. Pervej, M. M. Hasan, "Effect of signal length in cross-correlation based underwater network size estimation," in Proc. International Conference on Electrical Engineering and Information Communication Technology (ICEEICT): 1-6, 2015.

[37] B. K. Dash, H. H. Raton, S. A. H. Chowdhury, S. A. Rahman, "Performance analysis of cross-correlation based underwater network node estimation technique by varying signal length," in Proc. International Conference on Advancement in Electrical and Electronic Engineering: 1-4, 2018.

[38] S. A. H. Chowdhury, J. E. Giti, M. S. Anower, "Transmit energy calculation in cross-correlation based underwater network cardinality estimation," in Proc. IEEE International WIE Conference on Electrical and Computer Engineering (WIECON-ECE): 362-365, 2015.

[39] S. A. H. Chowdhury, M. S. Anower, J. E. Giti, M. I. Haque, "Effect of signal strength on different parameters of cross-correlation function in underwater network cardinality," in Proc. 2014 17th International Conference on Computer and Information Technology (ICCIT), 2014.

[40] M. S. Anower, S. A. H. Chowdhury, J. E. Giti, "Mitigating the effect of multipath using cross-correlation: application to underwater network cardinality estimation," Int. J. Syst., Control Commun., 7(3): 197-220, 2016.

[41] M. S. Anower, S. A. H. Chowdhury, J. E. Giti, "A robust signal processing approach of underwater network size estimation taking multipath propagation effects into account," Adv. in Netw., 3(3): 22-32, 2015.

[42] H. Sarker, M. Oli-Uz-Zaman, I. H. Chowdhury, S. A. H. Chowdhury, M. R. Islam, "Node estimation approach of underwater communication networks using cross-correlation for direct and multi-path propagation," in Proc. International Conference on Robotics,Electrical and Signal Processing Techniques (ICREST): 286-291, 2019.

[43] M. K. Hossain, M. S. Anower, M. M. Rahman, S. M. N. Siraj, "Effect of dispersion coefficient on underwater network size estimation," in Proc. International Conference on Electrical Engineering and Information Communication Technology (ICEEICT): 1-4, 2015.

[44] M. S. Anower, S. A. H. Chowdhury, J. E. Giti, M. I. , Haque"Effect of correlation based underwater network size -bandwidth in cross ,estimation" in .Proc8th International Conference on Electrical and Computer Engineering: 413-416, 2014.

[45] S. K. Bain, S. A. H. Chowdhury, A. H. M. Asif, M. S. Anower, M. F. Pervej, S. S. Haque, "Impact of underwater bandwidth on cross-correlation based node estimation technique," in Proc. 2014 17th International Conference on Computer and Information Technology (ICCIT), 2014.

[46] H. H. Raton, S. A. H. Chowdhury, M. J. Rana, M. S. Anower, S. A. Hossain, M. I. Sarkar, "Cross-correlation based approach of underwater network cardinality estimation with random placement of sensors," in Proc. IEEE International Conference on Telecommunications and Photonics (ICTP): 1-5, 2015.

[47] D. K. Mondal, S. A. H. Chowdhury, Q. N. Ahmed, M. S. Anower, "Cross-correlation based approach of underwater network size estimation with unequal sensor separation," in Proc. International Conference on Computer and Information Engineering (ICCIE): 99-102, 2015.

[48] B. K. Dash, S. A. H. Chowdhury, A. H. M. M. Kamal, M. S. Anower, A. Halder, "Underwater network cardinality estimation using cross-correlation: Effect of unequal sensor spacing," in Proc. International Workshop on Computational Intelligence (IWCI): 181-186, 2016.

[49] M. S. Anower, "Estimation using cross-correlation in a communications network," Ph.D. dissertation, SEIT, University of New South Wales at Australian Defense Force Academy, Canberra, 2011.

[50] M. S. , AnowerS. A. H. , ChowdhuryJ. E. , GitiA. S. M. , SayemM. I. ,Haque"Underwater network size estimation estimation using ,correlation: selection of estimation parameter-cross" in Proc. 9th 9th International Forum on Strategic Technology (IFOST), 2014.

[51] S. W. Smith, "Chapter 2: Statistics, probability and noise," in The Scientist and Engineer's Guide to Digital Signal Processing, California Technical Publishing, San Diego, CA, 1999.

[52] S. A. H. ,ChowdhuryM. S. , AnowerJ. E. ,Giti"Performance comparison of underwater network size estimation techniques," Int. J. Syst., Control Commun., 7 (1): 16-34, 2016.

[53] S. A. H. Chowdhury, J. E. Giti, M. S. Anower, "Optimization between estimation error and transmit energy in cross-correlation based underwater network cardinality estimation," Wireless Pers. Commun., 97: 5797-5816, 2017.

[54] M. S. A. Howlader, "Estimation and identification of neighbours in wireless networks considering the capture effect and long delay," Ph.D. dissertation, SEIT, University of New South Wales at Australian Defense Force Academy, Canberra, 2009.

[55] B. A. Barry, "Errors in practical measurement in science, engineering, and technology," John Wiley & Sons, Hoboken, New Jersey, 1978.

Biographies

Md. Zillur Rahman received his B.Sc. degree in Electrical & Electronic Engineering from the Rajshahi University of Engineering & Technology, Rajshahi, Bangladesh, in 2012. His research interests are Signal Processing and Underwater Communication. Currently, he is pursuing M.Sc. degree in the department of Electrical & Electronic Engineering at the Rajshahi University of Engineering & Technology, Rajshahi, Bangladesh.

- Email: zillur.eee07@gmail.com
- ORCID: NA
- Web of Science Researcher ID: NA
- Scopus Author ID: NA
- Homepage: NA

Jishan E Giti obtained her Ph.D. degree from the Monash University, Australia in 2020. She received her B.Sc. and M.Sc. degrees in Electrical & Electronic Engineering from the Rajshahi University of Engineering & Technology, Rajshahi, Bangladesh, in 2011 and 2014, respectively. Her major research interests are Physical Layer Security, Wireless Communication and Networking. Currently, she is serving as an Associate Professor in the department of Electrical & Electronic Engineering at the Rajshahi University of Engineering & Technology, Rajshahi, Bangladesh.

- Email: jishan.e.giti@gmail.com, jishan@eee.ruet.ac.bd
- ORCID: 0000-0001-5286-5450
- Web of Science Researcher ID: NA
- Scopus Author ID: NA
- Homepage: https://www.ruet.ac.bd/jishan

Shah Ariful Hoque Chowdhury obtained his Ph.D. degree from the Australian National University, Australia in 2021**.** He received his bachelor's degree in Electronics & Telecommunication Engineering and master's degree in Electrical & Electronic Engineering from the Rajshahi University of Engineering & Technology, Rajshahi, Bangladesh, in 2011 and 2014, respectively. His research fields are Underwater Communication, Wireless Communication and Computer Vision. Currently, he is serving as a Professor in the department of Electronics & Telecommunication Engineering at the Rajshahi University of Engineering & Technology, Rajshahi, Bangladesh.

- Email: arif.1968.ruet@gmail.com, ariful.hoque@ete.ruet.ac.bd
- ORCID: 0000-0003-2597-156X
- Web of Science Researcher ID: NA
- Scopus Author ID: NA
- Homepage: https://www.ruet.ac.bd/ariful

Md. Shamim Anower was born on 5th October 1977 in Bangladesh. He obtained his Ph.D. degree from the University of New South Wales, Australia in 2012**.** He received his B.Sc. and M.Sc. degrees in Electrical & Electronic Engineering from the Rajshahi University of Engineering & Technology in 2002 and 2007, respectively. His major research interests are Underwater Wireless Communication, Power Line Communication, Signal Processing for Communications, Power System Analysis and Stability Enhancement. He published more than 100 international and national journal and conference articles so far. Currently, he is serving as a Professor in the department of Electrical & Electronic Engineering at the Rajshahi University of Engineering & Technology, Rajshahi, Bangladesh.

- Email: md.shamimanower@yahoo.com, msanower@eee.ruet.ac.bd
- ORCID: 0000-0001-6986-6847
- Web of Science Researcher ID: NA
- Scopus Author ID: NA
- Homepage: https://www.ruet.ac.bd/Shamim

How to cite this paper:
M. Zillur Rahman, J. E Giti, S. Ariful Hoque Chowdhury, M. Shamim Anower, "Cross-correlation based approach for counting nodes of undersea communications network considering limited bandwidth," J. Electr. Comput. Eng. Innovations, 13(1): 241-256, 2025.

DOI: 10.22061/jecei.2024.11252.783

URL: https://jecei.sru.ac.ir/article_2230.html